Available online at www.sciencedirect.com
ScienceDirect
Bioelectrochemistry 70 (2007) 2–11
Bioelectrochemistry
www.elsevier.com/locate/bioelechem

Review

Biomolecule–nanoparticle hybrid systems for bioelectronic applications

Itamar Willner *, Bilha Willner, Eugenii Katz

Institute of Chemistry, The Hebrew University of Jerusalem, Jerusalem 91904, Israel

Received 14 July 2005
Available online 5 June 2006

Abstract

Recent advances in nanobiotechnology involve the use of biomolecule–nanoparticle (NP) hybrid systems for bioelectronic applications. This is exemplified by the electrical contacting of redox enzymes by means of Au-NPs. The enzymes, glucose oxidase, GOx, and glucose dehydrogenase, GDH, are electrically contacted with the electrodes by the reconstitution of the corresponding apo-proteins on flavin adenine dinucleotide (FAD) or pyrroloquinoline quinone (PQQ)-functionalized Au-NPs (1.4 nm) associated with electrodes, respectively. Similarly, Au-NPs integrated into polyaniline in a micro-rod configuration associated with electrodes provides a high surface area matrix with superior charge transport properties for the effective electrical contacting of GOx with the electrode. A different application of biomolecule–Au-NP hybrids for bioelectronics involves the use of Au-NPs as carriers for a nucleic acid that is composed of hemin/G-quadruplex DNAzyme units and a detecting segment complementary to the analyte DNA. The functionalized Au-NPs are employed for the amplified DNA detection, and for the analysis of telomerase activity in cancer cells, using chemiluminescence as a readout signal.

Biomolecule–semiconductor NP hybrid systems are used for the development of photoelectrochemical sensors and optoelectronic systems. A hybrid system consisting of acetylcholine esterase (AChE)/CdS–NPs is immobilized in a monolayer configuration on an electrode. The photocurrent generated by the system in the presence of thioacetylcholine as substrate provides a means to probe the AChE activity. The blocking of the photocurrent by 1,5-bis(4-allyldimethyl ammonium phenyl)pentane-3-one dibromide as nerve gas analog enables the photoelectrochemical analysis of AChE inhibitors. Also, the association CdS–NP/double-stranded DNA hybrid systems with a Au-electrode, and the intercalation of methylene blue into the double-stranded DNA, generates an organized nanostructure of switchable photoelectrochemical functions. Electrochemical reduction of the intercalator to the leuco form, −0.4 V vs. SCE, results in a cathodic photocurrent as a result of the transfer of photoexcited conduction-band electrons to O_2 and the transport of electrons to the valance-band holes by the reduced intercalator units. The oxidation of the intercalator, E 0 V (vs. SCE), yields in the presence of triethanolamine, TEOA, as sacrificial electron donor, an anodic photocurrent by the transport of conduction-band electrons, through intercalator units, to the electrodes, and filling the valance-band holes with electrons supplied by TEOA. The systems reveal potential-switchable directions of the photocurrents, and reveal logic gate functions.

Keywords: Nanobiotechnology; Nanoparticles; Enzymes; DNA; Electrochemistry; Photoelectrochemistry

Biomaterials such as enzymes, antigens/antibodies, receptors or folded DNA, exhibit nanometric sizes, comparable to those of nano-objects such as nanoparticles, nanorods, or nanowires. Thus, by the integration of biomolecules with nanosized materials one may yield hybrid materials that combine the evolutionary optimized recognition and catalytic properties of biomaterials with the unique electronic, optical and catalytic functions of nanomaterials. Indeed, substantial research efforts were recently directed to use biomolecule–nanoparticle hybrid systems to tailor novel bioelectronic systems that may be applied in the design of biosensors, the fabrication of electronic nanocircuitry, and even the development of nanodevices [1,2]. The present paper summarizes some of our recent accomplishments in the field of nanobiotechnology by describing some examples that demonstrate how nanotechnology, and particularly metal and semiconductor nanoparticles, may be harnessed to resolve fundamental aspects in bioelectrochemistry.

1. Electrical contacting of redox proteins by means of Au-nanoparticles (NPs)

The lack of direct electrical communication between redox proteins and electrode supports is a fundamental phenomenon that

* Corresponding author. Tel.: +972 2 6585272; fax: +972 2 6527715.
E-mail address: willnea@vms.huji.ac.il (I. Willner).

1567-5394/$ - see front matter © 2006 Elsevier B.V. All rights reserved.
doi:10.1016/j.bioelechem.2006.03.013

limits the use of redox enzymes in biosensors or biofuel cells design. It originates from the spatial separation of the redox-active sites embedded in the protein matrices from the electrode surfaces [3]. Numerous methods to electrically communicate redox enzymes with electrodes were developed, including the application of diffusional electron mediators [4], tethering redox-relays to the proteins [5–7] and the immobilization of redox proteins in electroactive polymers [8–10]. A recently developed procedure for the electrical contacting of redox proteins with electrodes has involved the extraction of the native redox cofactor from the protein, and the reconstitution of the resulting apo-enzyme on a surface modified with a monolayer consisting of a relay tethered to the respective cofactor unit [11–14]. The reconstitution process aligned the protein on the electrode surface in an optimal orientation, while the relay units electrically communicated the cofactor sites with the conductive support, and this enabled the bioelectrocatalytic activation of the respective enzymes.

Functionalized Au-nanoparticles (Au-NPs) were used as nano-electrodes to align and electrically contact redox enzymes with electrode supports, Scheme 1. Functionalized Au-NPs, 1.4 nm, were linked to a gold electrode by means of a 1,4-benzenedithiolate linker (1). The respective cofactor was then covalently linked to the Au-NP, and the respective apo-enzyme was reconstituted onto the cofactor units to yield the electrically contacted enzyme electrode. The flavoenzyme glucose oxidase, GOx, was electrically contacted by this method [15]. The synthetic amine-tethered flavin adenine dinucleotide cofactor, FAD–NH_2 (2), was linked to the active-ester-functionalized Au-NPs (3) associated with the electrode, and apo-GOx was reconstituted on the FAD sites. Fig. 1(A) shows the cyclic voltammograms of the reconstituted enzyme electrode in the presence of variable concentrations of glucose. The observed electrocatalytic anodic currents indicate that the reconstituted enzyme reveals electrical communication between its active site and the electrode. The magnitudes of the electrocatalytic anodic currents are controlled by the concentration of glucose, and the corresponding calibration curve is depicted in Fig. 1(A), inset. Knowing the surface coverage of the reconstituted enzyme (1×10^{-10} mol cm^{-2}), and the maximum current density extracted from the system, the electron transfer turnover rate between the cofactor site and the electrode was estimated to be ca. $k_{et}\approx5000\ s^{-1}$. This value is ca. 7-fold higher than the turnover rate of electrons between the active site of the native enzyme and its native acceptor, oxygen [16]. This unprecedented effective electrical contact between GOx and the electrode was attributed to the intimate contact between the Au-NP and the redox cofactor that stimulates the effective electron transport to the electrode by means of the Au-NP, acting as a nano-electrode. The effective electrical communication between the enzyme and the electrode reveals a new paradigm to harness nanotechnology for bioelectrochemical functions. Besides the fundamental significance of the method it has important practical implications, as it suggests that enhanced sensitivities, miniaturization of the electrodes, and screening of non-specific oxidizable interfering substances may be accomplished by this nano-engineered enzyme electrode. Indeed, it was demonstrated that amperometric responses of the GOx-reconstituted electrode were insensitive to O_2 or common glucose sensing interferants such as ascorbate.

A similar concept was applied to electrically contact the pyrroloquinoline quinone (PQQ)-dependent glucose dehydrogenase [17]. Apo-glucose dehydrogenase (apo-GDH) was

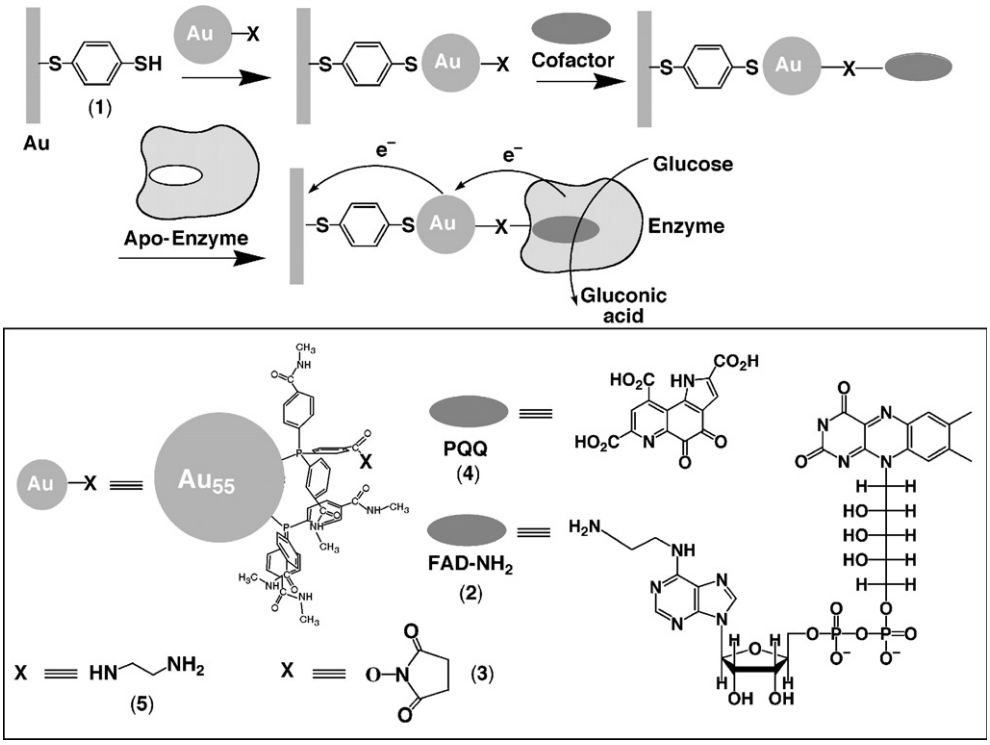

Scheme 1. Electrical wiring of enzymes by the reconstitution of apo-enzymes on the cofactor-functionalized Au nanoparticles associated with electrodes.

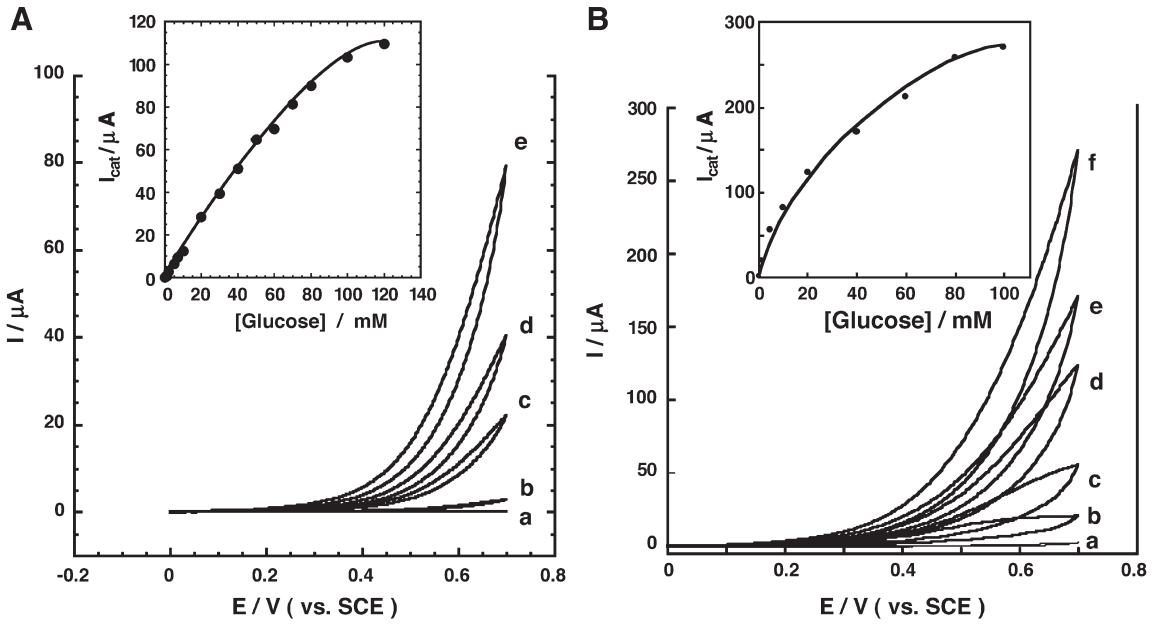

Fig. 1. (A) Cyclic voltammograms corresponding to the bioelectrocatalyzed oxidation of glucose by GOx reconstituted on the FAD-functionalized Au-NPs associated with a Au electrode in the presence of different concentrations of glucose: (a) 0 mM, (b) 1 mM, (c) 10 mM, (d) 20 mM, and (e) 50 mM. Results were recorded in 0.1 M phosphate buffer (pH 7.0), under Ar, potential scan rate 5 mV s^{-1}. Inset: Calibration plot derived from the cyclic voltammograms at E=0.6 V. (B) Cyclic voltammograms corresponding to the bioelectrocatalyzed oxidation of glucose by the GDH reconstituted on the PQQ-functionalized Au-NPs associated with a Au electrode in the presence of different concentrations of glucose: (a) 0 mM, (b) 1 mM, (c) 5 mM, (d) 20 mM, (e) 40 mM and (f) 100 mM. The data were recorded in 0.1 M phosphate buffer, pH=7.3, under Ar, potential scan rate 5 mV s^{-1}. Inset: Calibration plot derived from the cyclic voltammograms at E=0.7 V.

reconstituted onto PQQ-cofactor units (4) covalently linked to the amino-functionalized Au-NPs (5), Scheme 1. Fig. 1(B) shows the electrocatalytic anodic currents developed by the enzyme-modified electrode in the presence of variable concentrations of glucose. The resulting electrocatalytic currents imply that the system is electrically contacted, and that the Au-NPs

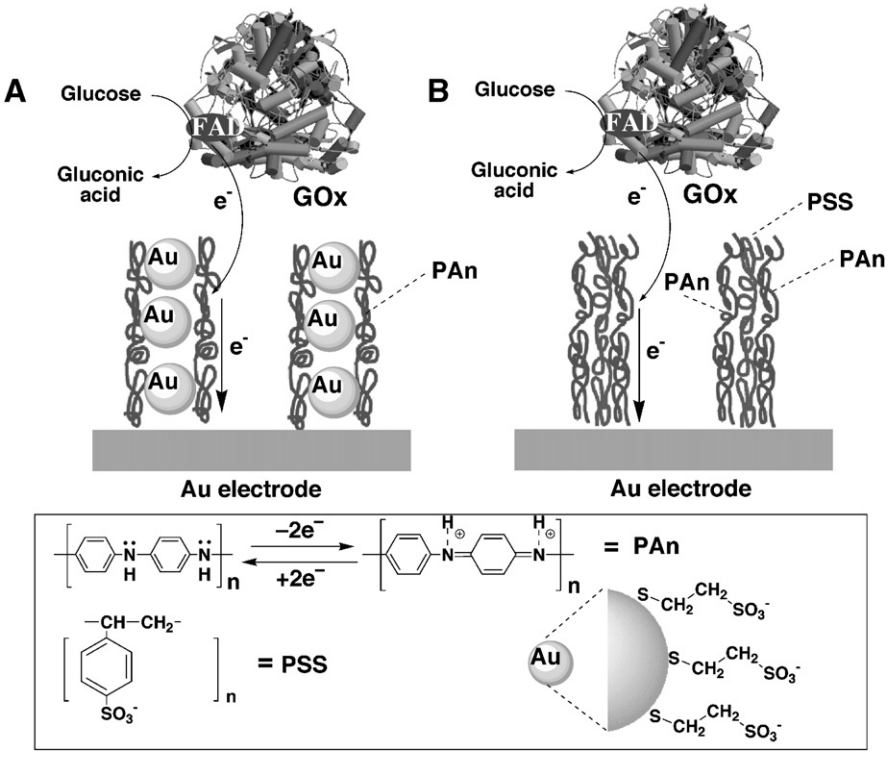

Scheme 2. Bioelectrocatalytic oxidation of glucose in the presence of GOx mediated by: (A) Polyaniline/Au-nanoparticles composite micro-rods. (B) Polyaniline/polystyrene sulfonate composite micro-rods.

mediate the electron transfer from the PQQ-cofactor center to the electrode. From the maximum value of the extracted current density, Fig. 1(B), inset, and knowing the surface coverage of the reconstituted enzyme, 1.4×10^{-10} mol cm^{-2}, the electron transfer turnover rate between the biocatalyst and the electrode was estimated to be 11,800 s^{-1}, a value that implies effective electrical communication between the enzyme and the electrode, that leads to the efficient bioelectrocatalytic oxidation of glucose. The reconstitution of redox enzymes on other cofactor-modified nano-objects, such as carbon nanotubes, was similarly used to electrically contact the redox biocatalyst and conductive supports [18].

Au-NPs may also be used to enhance charge transport through conductive matrices, and thereby accelerate bioelectrocatalytic processes. This has been demonstrated by the application of polyaniline micro-rods that include Au-NPs and are associated with a bulk electrode surface as an organized matrix for the activation of bioelectrocatalytic processes [19]. The Au-NP/polyaniline composite, Au-NP/PAn, micro-rods were prepared and used to mediate glucose oxidation in the presence of GOx as outlined in Scheme 2(A). A porous alumina membrane (0.2 μm pore size) was coated from one side with a Au layer. Au-NPs (ca. 4 nm) functionalized with a capping layer, consisting of 2-mercaptoethane sulfonic acid, were incorporated into polyaniline in the membrane pores. The subsequent dissolution of the membrane template yielded rods on the electrode that were ca. 350–850 nm long and 200 μm thick (due to the swelling of the polymer generated in the pores). The resulting polymer revealed quasi-reversible electrochemical properties at neutral pH values due to the negative capping layer that protects the Au-NPs. For comparison, micro-rods consisting of a composite of polyaniline/polystyrene sulfonate, PAn/PSS, were prepared and used to mediate glucose oxidation in the presence of GOx, Scheme 2(B) [19]. The Au-NPs/PAn composite in the micro-rod configuration has important advantages as tailored matrix for the activation of bioelectrocatalytic transformations: (i) the charge transport through the Au-NPs/PAn composite was found to be substantially faster than in the PSS/PAn system. Chronoamperometric experiments following the oxidation of the polyaniline rods revealed that it was 25-fold faster in the Au-NPs/PAn assembly than in the PAn/PSS rod material. These enhanced charge transport features of the Au-NPs/PAn hybrid material were attributed to electron hopping through the Au-NPs, a process that facilitates charge migration. (ii) The micro-rod structure of the Au-NPs/PAn conducting polymer provides a high surface area interface, and thus the electrical contacting of a solution-solubilized enzyme should be facilitated. The cyclic voltammograms corresponding to the Au-NPs/PAn or PAn/PSS-mediated oxidation of glucose by glucose oxidase, GOx, are depicted in Fig. 2(A) and (B),

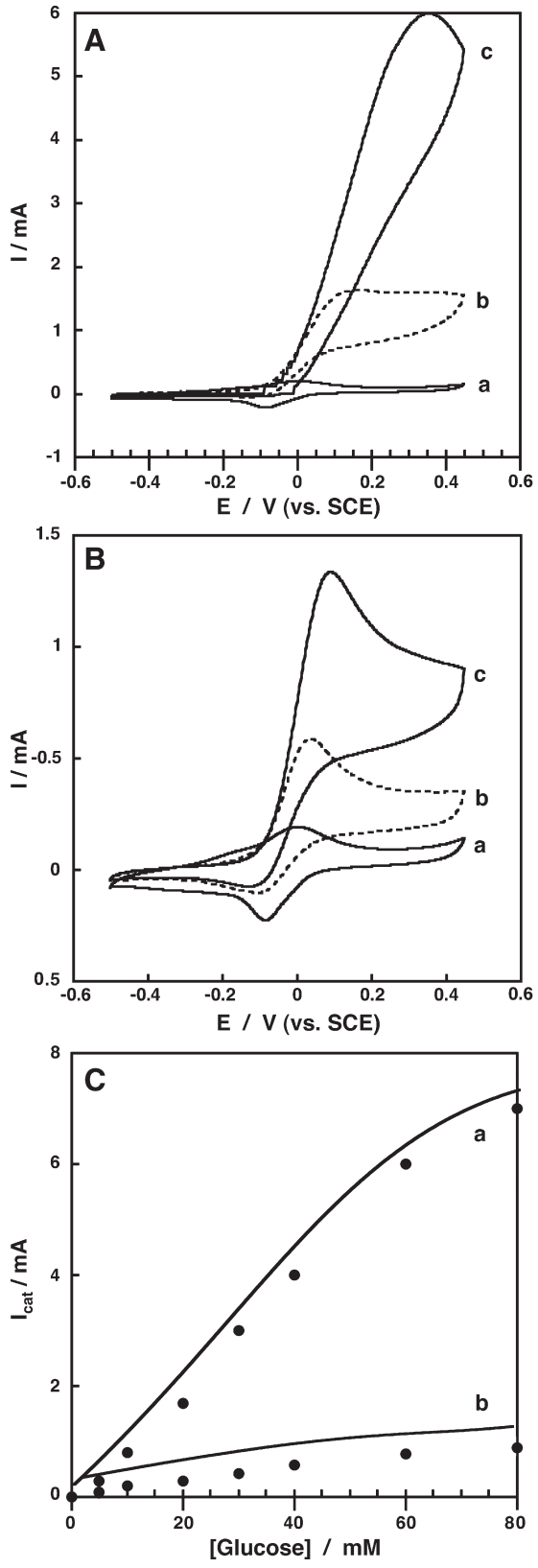

Fig. 2. Bioelectrocatalytic oxidation of glucose by solubilized GOx, 1 mg mL^{-1}, and mediated by the microstructured redox-active rod assemblies: (A) Cyclic voltammograms recorded in the presence of the microstructured assemblies composed of PAn/Au-NPs and different concentrations of glucose: a) 0 mM, b) 10 mM, c) 60 mM. (B) Cyclic voltammograms recorded in the presence of the microstructured assemblies composed of PAn/PSS and different concentrations of glucose: a) 0 mM, b) 10 mM, c) 60 mM. (C) Calibration plots derived from the cyclic voltammograms at $E=0.4$ V: a) for the PAn/Au-NPs system, b) for the PAn/PSS system. The data were recorded in 0.1 M phosphate buffer, pH=7.5. Oxygen was removed from the background solution by bubbling Ar. Potential scan rate, 5 mV s^{-1}.

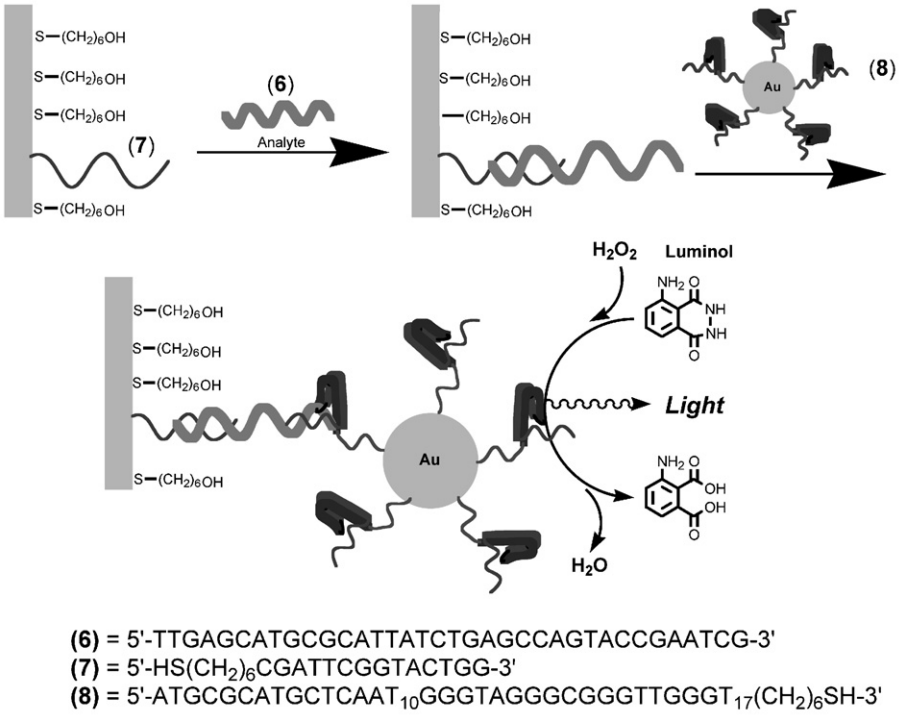

(6) = 5'-TTGAGCATGCGCATTATCTGAGCCAGTACCGAATCG-3'
(7) = 5'-HS$(CH_2)_6$CGATTCGGTACTGG-3'
(8) = 5'-ATGCGCATGCTCAAT_{10}GGGTAGGGCGGGTTGGGT$_{17}(CH_2)_6$SH-3'

Scheme 3. Amplified chemiluminescence detection of DNA using DNAzyme-functionalized Au-NPs.

respectively. The electrocatalytic anodic currents indicate that the bioelectrocatalyzed oxidation of glucose proceeds effectively in the two systems. The anodic currents in the Au-NP/PAn system are, however, 4-fold higher as compared to the anodic currents in the analogous PAn/PSS systems, revealing improved bioelectrocatalytic activity of the former system, Fig.2(C). The higher bioelectrocatalytic functions of the Au-NP/PAn assembly were attributed to the enhanced charge transport properties of the Au-NPs/polymer matrix that facilitates the electrical contact between the enzyme units and the electrode.

2. Au-NPs as carriers for DNAzymes for the amplified detection of DNA and telomerase activity

The synthesis of aptamers and catalytic nucleic acids (DNAzymes) became a common practice in nucleic acid chemistry and biocatalysis [20–22]. Among numerous catalytic

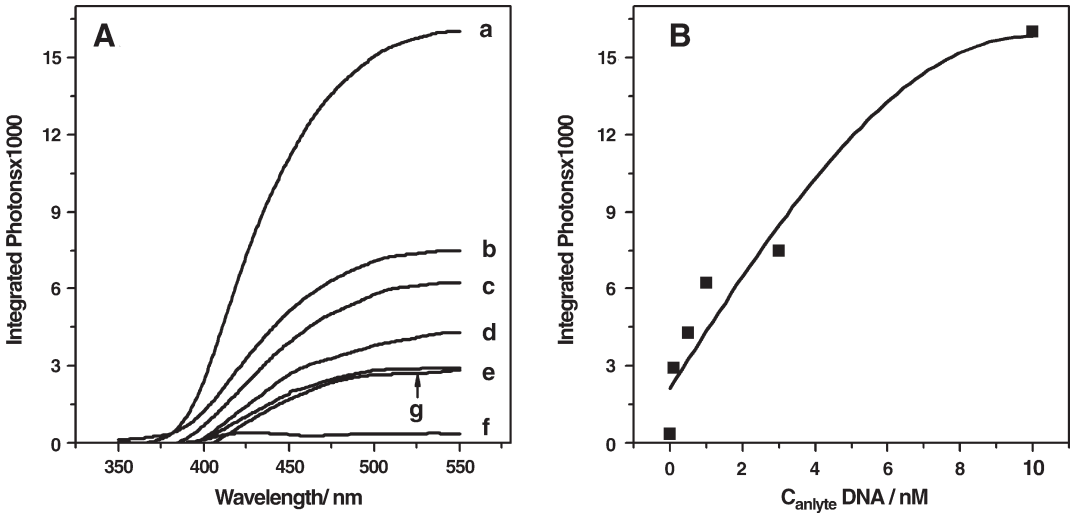

Fig. 3. (A) Integrated light intensities observed upon the analysis of different concentrations of DNA (6) by the DNAzyme (8)-modified Au-NPs: (a) 10 nM; (b) 5 nM; (c) 1 nM; (d) 0.5 nM;(e) 0.1 nM; (g) 1 nM, while using free DNAzyme (8) (unbound to the Au-NPs) 2.5 μM, as a label. (f) The analysis of 6 without added DNAzyme-functionalized Au-NPs but upon treatment with hemin 2.5 μM. In all experiments the analyzing solution consisted of a buffer solution, pH=9.0, composed of 25 mM HEPES-buffer, 20 mM KCl, 200 mM NaCl, 0.05% Triton X-100 and 1% DMSO, that included 0.5 mM luminol and 30 mM H_2O_2. (B) Calibration curve corresponding to the analysis of DNA (6) by the DNAzyme (8)-functionalized Au-NPs.

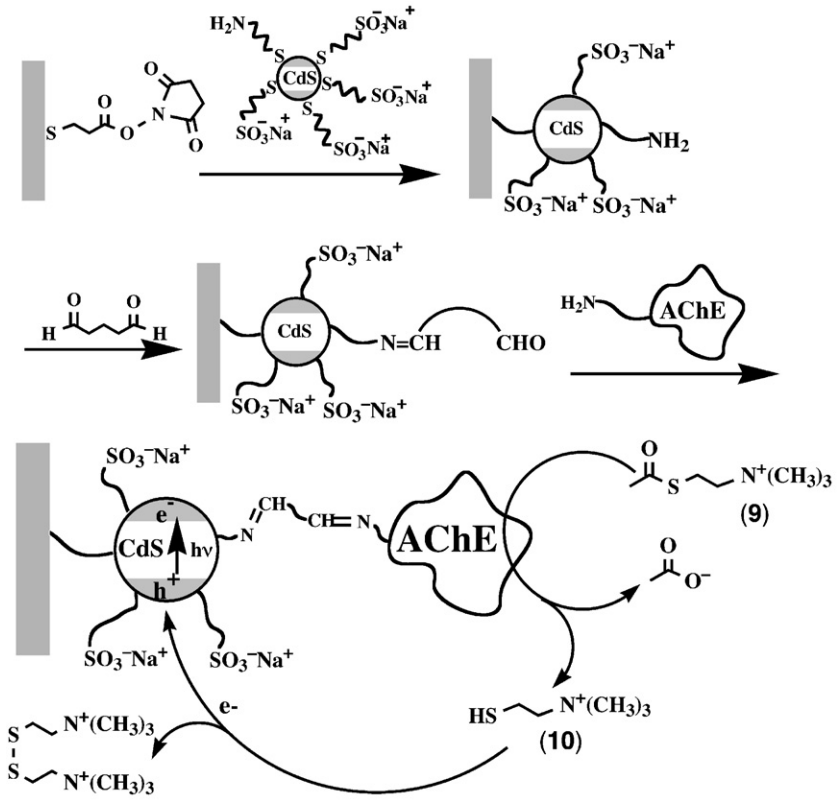

Scheme 4. Assembly of the CdS nanoparticle/AChE hybrid system used for the photoelectrochemical detection of the AChE activity and its inhibition.

DNAs developed to date a nucleic acid sequence, that forms a G-quadruplex structure that binds hemin, was found to exhibit horseradish peroxidase (HRP)-like activities [23,24]. It was reported that the hemin/G-quadruplex catalyzes the H_2O_2-mediated oxidation of the dye 2,2′-azino-bis(3-ethylbenzthiazoline-6-sulfonic acid) diammonium salt (ABTS). Thus, DNAzymes may be used as catalytic labels for the amplified analysis of biorecognition events. Indeed, a DNA "hairpin" structure that included the hemin/quadruplex DNAzyme was employed for the amplified detection of DNA via the biocatalytic process [25]. We have further demonstrated [26] that the hemin/G-quadruplex complex catalyzes the generation of chemiluminescence in the presence of H_2O_2 and luminol.

We have used Au-NPs as carriers for the DNAzyme units and employed the functionalized NPs for the amplified detection of DNA [27]. Scheme 3 shows the method to analyze a DNA (6) by the DNAzyme label. The thiolated nucleic acid (7) was assembled on a Au surface, and it acts as the sensing interface for 6. The sensing nucleic acid hybridizes with one end of the target DNA, (6). The Au-NPs were functionalized with the DNAzyme consisting of the hemin/G-quadruplex complex (8) tethered to a nucleic acid residue that is complementary to a part of the single-stranded domain of 6 associated with the interface. The Au-NPs were modified with ca. 96 units of the bifunctional nucleic acid (8) that includes the recognition site (for hybridization with 6) and the catalytic DNAzyme label. The interface with the hybridized (7)/(6) duplexes was then reacted with the DNAzyme-functionalized Au-NPs. Since each particle carries many DNAzyme units, a single recognition event of 6 results in the coupling of numerous DNAzyme conjugates that lead to the generation of chemiluminescence. Fig. 3 shows the integrated light intensity observed upon the analysis of different concentrations of the DNA (6). The method has enabled the analysis of the DNA with a sensitivity limit corresponding to 1×10^{-10} M. This method was further

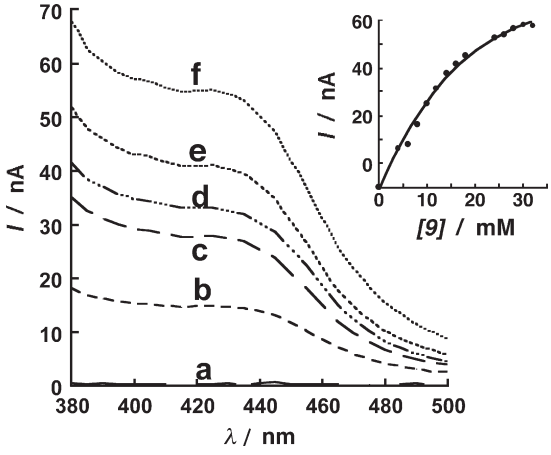

Fig. 4. Photocurrent action spectra observed in the presence of acetylthiocholine (9): (a) 0 mM, (b) 6 mM, (c) 10 mM, (d) 12 mM, (e) 16 mM, (f) 30 mM. (Inset) Calibration curve corresponding to the photocurrent at λ=380 nm at variable concentrations of 9. Spectra were recorded in 0.1 M phosphate buffer, pH) 8.1, under argon.

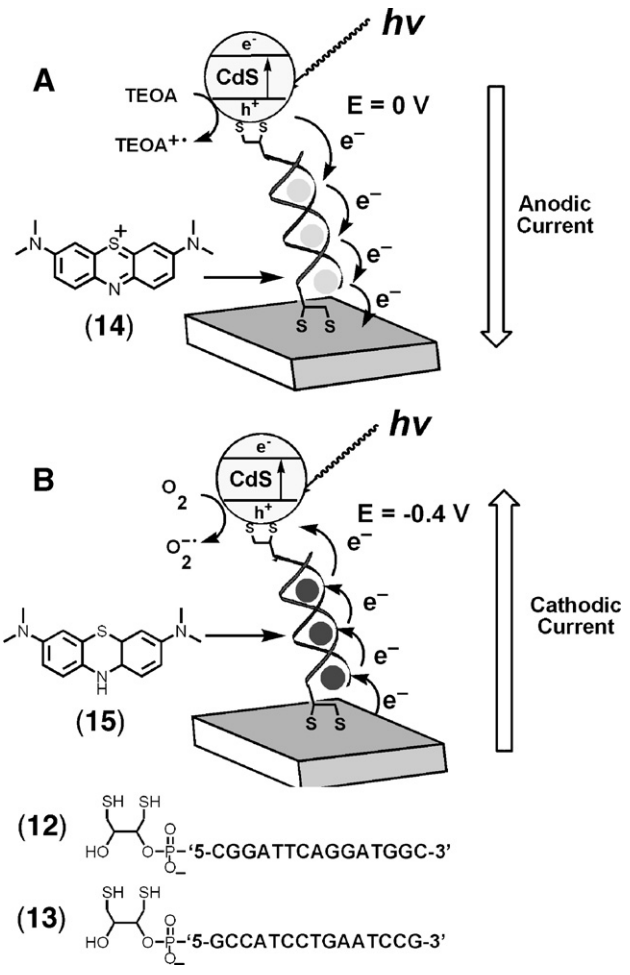

Scheme 5. Directional electroswitchable photocurrents in the CdS-NPs/ds-DNA/intercalator system. (A) Enhanced generation of anodic photocurrent in the presence of the oxidized methylene blue intercalator (14) (applied potential $E=0$ V). (B) Enhanced generation of cathodic photocurrent in the presence of the reduced methylene blue intercalator (15) (applied potential $E=-0.4$ V).

developed for the analysis of telomerase activity in HeLa cancer cells.

3. Biomolecule/semiconductor quantum dots for photoelectrochemical applications

Semiconductor quantum dots (QDs) reveal unique size-controlled absorbance and fluorescence properties [28]. Photoexcitation of the semiconductor quantum dots yields the transfer of an electron from the semiconductor valence-band to its conduction-band, to yield an electron-hole pair. The electron-hole recombination in the QD may either lead to thermal relaxation of the excited species, or yield light emission from the particle. Indeed, the luminescent properties of semiconductor QDs are broadly used for imaging of biorecognition events [29,30]. Also, the photonic properties of semiconductor quantum dots were recently applied to develop sensing routes of higher complexity, whereby the semiconductor QDs were used as optical activating units for fluorescence resonance energy transfer (FRET) to dye units that follow DNA detection processes [31].

The coupling of semiconductor quantum dots to electrode supports enables, upon excitation of the QD, a further photophysical path, namely, the generation of photocurrent through the primary excitation of the semiconductor NPs. The conjugation of biomolecules with semiconductor NPs, and the coupling of the biomolecule/NP hybrids to electrodes may then lead to photoelectrochemical phenomena that follow biological transformations, thus, establishing the area of photobioelectrochemistry in nanostructure systems. Although the development of photoelectrochemically-active biomolecule/semiconductor NP hybrid systems is at its infancy, some recent activities highlight the future perspectives of these systems in bioelectrochemistry. We address in the present discussion the development of an enzyme/semiconductor–NP conjugate that can be used for the development of a photoelectrochemically-based sensor. Also, the assembly of DNA/semiconductor QDs on electrodes is described, and the electronic properties of the system are discussed.

CdS–NPs (diameter ca. 3 nm), capped with a protecting monolayer of cysteamine and mercaptoethane sulfonic acid, were covalently linked to a cysteic acid monolayer-functionalized electrode, and then the enzyme acetylcholine esterase, AChE, was coupled to the NPs to yield the enzyme/NP conjugate on the electrode, Scheme 4, [32]. Photoexcitation of this system does not lead to the formation of a net photocurrent since the photogenerated electron-hole pairs recombine. Addition of acetylthiocholine (9) to the system results in the AchE-mediated hydrolysis of 9 to thiocholine (10) and acetate. Thiocholine (10) is, however, an electron donor, that is oxidizable by the valence-band holes. The photogenerated electron-hole pair may be scavenged by the concomitant oxidation of 10 by valence-band holes, and this results in the transfer of the conduction-band electrons to the electrode, thus generating a steady-state photocurrent [32]. Fig. 4, curves (a)–

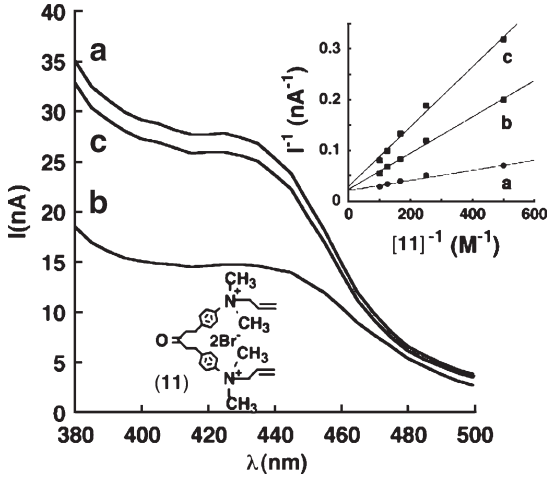

Fig. 5. Photocurrent spectra corresponding to the CdS/AChE system in the presence of 9, 10 mM, (a) without the inhibitor, (b) upon addition of 11, 10 μM, (c) after rinsing the system and excluding the inhibitor. Inset: Lineweaver–Burk plots corresponding to the photocurrent at variable concentrations of 9, in the presence of 11: (a) 0 μM, (b) 10 μM, (c) 20 μM. Data were recorded in 0.1 M phosphate buffer, pH=8.1, under argon.

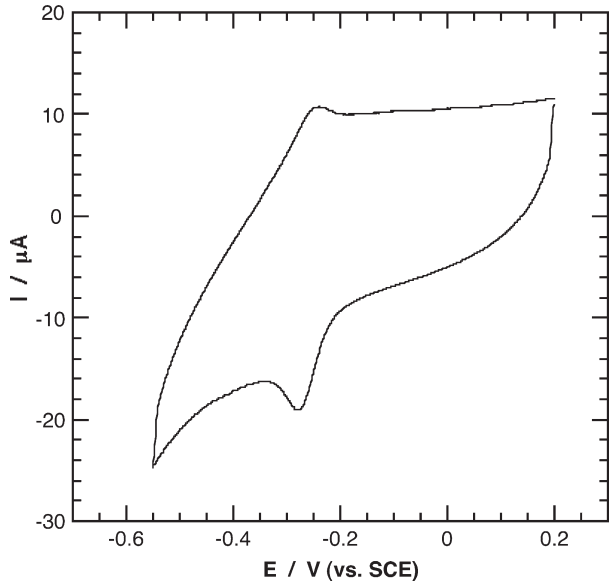

Fig. 6. Cyclic voltammmogram of methylene blue intercalated into the ds-DNA assembly. Potential scan rate 50 mV s^{-1}.

(f), shows the photocurrent action spectra observed upon irradiation of the modified electrode in the presence of variable concentrations of 9. As the concentration of 9 is elevated, the photocurrent intensities are enhanced, since higher amounts of the electron donor (10) are formed by the biocatalytic process, thus improving the scavenging of the valence-band holes and increasing the steady-state photocurrents, Fig. 4, inset. The photocurrent action spectra follow the absorbance features of the CdS–NPs, implying that the photocurrents originate from the excitation of the CdS–NPs. Acetylcholine is a central neurotransmitter that activates the synapse and the neural response. The neurotransmitter, after activating the neural system, is rapidly hydrolyzed by the serine protease AChE to restore the resting potential of the synaptic membrane. Different reagents, such as the nerve gas diisopropyl fluorophosphate (Sarin) or toxins (e.g., cobratoxin) act as inhibitors of AChE. Blocking of the enzyme-stimulated nerve conduction leads to rapid paralysis of vital functions of living systems. Thus, the assembly described here may be further developed to a biomaterial–semiconductor hybrid system for biosensing of biological warfare. Fig. 5 shows the photocurrent spectra of the system before addition of the inhibitor, curve (a), and in the presence of 1,5-bis(4-allyldimethylammoniumphenyl)pentane-3-one dibromide (11), 10 mM, curve (b), that is used as a model compound for the inhibition of AChE [33]. The observed decrease in the photocurrents was attributed to the inhibition of the biocatalyst, a process that retards the biocatalyzed generation of the hole-scavenging electron donor (10). Fig. 5, inset, shows the analysis of the inhibition process of AChE by 11 following the decrease of the photocurrent in the system. The resulting Lineweaver–Burk plot indicates that 11 inhibits the biocatalyst by a competitive mechanism, $K_I = 7$ μM. The rinsing of the electrode with a buffer solution washed off the inhibitor (11), and the original photocurrent of the modified electrode was regenerated, Fig. 5, curve (c).

A different biomolecule–semiconductor NP-based photoelectrochemical system involves a CdS–NPs layer linked to a Au support by a duplex DNA, and the study of the effect of a redox intercalator on the resulting photocurrent and its direction was performed [34]. The dithiol-tethered single-stranded (ss)-DNA (12) was assembled on a Au electrode, and CdS–NPs functionalized with the dithiol-tethered complementary nucleic acid (13) (ca. 3 nucleic acid residues per NP) were hybridized with the nucleic acid (12) associated with the electrode resulting in the double-stranded (ds)-DNA assembly, Scheme 5. The irradiation of the ds-DNA/CdS–NPs-modified electrode in the presence of triethanolamine (TEOA) as electron donor resulted in the anodic photocurrent. The conductivity through DNA has been a subject of substantial controversy in the recent years [35]. The observed generated photocurrent in the present system could imply electron transfer through the DNA matrix. Nonetheless, we believe that the imperfect structure of the CdS–NPs/DNA duplex is the origin for the photocurrent (vide infra). That is, the CdS–NPs/DNA duplexes generate a non-densely packed interface that enables the tilting of the monolayer components in respect to the electrode surface. The intimate contact between the CdS–NPs and the electrode support may then lead to the photocurrent. That is, the photoexcitation of the semiconductor NPs results in the generation of an electron-hole pair. The oxidation of the electron donor (TEOA) by the valence-band holes with

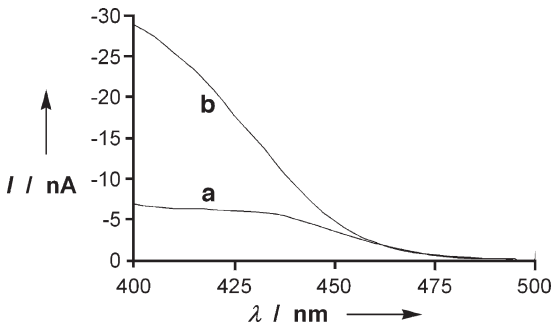

Fig. 7. Cathodic photocurrents generated in the CdS-NP/ds-DNA system associated with the electrode: (a) in the absence and (b) in the presence of reduced methylene blue intercalator (15). The data were obtained at the applied potential $E = -0.4$ V and in the presence of O_2 (under equilibrium with air).

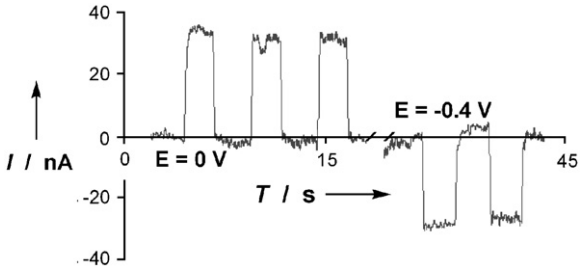

Fig. 8. Electrochemically switched anodic and cathodic photocurrents generated in the Cd-NPs/ds-DNA/14/15 systems at 0 and −0.4 V, respectively, in the presence of TEOA, 20 mM and O_2 (under equilibrium with air). Photocurrents were generated upon irradiation of $\lambda = 420$ nm.

the concomitant transfer of the conduction-band electrons to the electrode leads to the steady-state photocurrent. Further experiments support the conclusion that the observed low photocurrents do not stem from charge transfer through the DNA, and reveal that under certain conditions the double-stranded DNA may act as template for charge transport that leads to enhanced photocurrents, and to the possibility to switch the photocurrent direction by means of the potential applied on the electrode [34]. Methylene blue (14) was intercalated into the (12/13)-ds-DNA coupled to the CdS–NPs, Scheme 5(A). Fig. 6 shows the cyclic voltammogram of the intercalated methylene blue. The quasi-reversible wave implies that at potentials $E > -0.28$ V (vs. SCE) the intercalator exists in its oxidized form (14), whereas at potentials $E < -0.28$ V (vs. SCE) the intercalator exists in its reduced leuco form (15). Coulometric analysis of the methylene blue redox wave, $E° = -0.28$ V (vs. SCE), knowing the surface coverage of the ds-DNA, indicates that ca. 2–3 intercalator units are associated with the double-stranded DNA. An anodic photocurrent was generated in the system in the presence of TEOA as electron donor and methylene blue intercalated into the ds-DNA, and while applying a potential of 0 V (vs. SCE) on the electrode. At this potential methylene blue exists in its oxidized state (14) that acts as an electron acceptor. The resulting photocurrent is ca. 4-fold higher than that recorded in the absence of the intercalator. The enhanced photocurrent is attributed to the trapping of conduction-band electrons by the intercalator units and their transfer to the electrode that is biased at 0 V, thus retaining the intercalator units in their oxidized form. The oxidation of TEOA by the valence-band holes leads then to the formation of the steady-state anodic photocurrent. Biasing the electrode at potential of −0.4 V (vs. SCE), a potential that retains the intercalator units in their reduced state (15) leads, however, to the blocking of the photocurrent in the presence of TEOA and under an inert argon atmosphere. This experiment reveals clearly that the oxidized intercalator moieties with the DNA matrix play a central role in the charge transport of the conduction-band electrons and the generation of the photocurrent. Fig. 7, curve (b) shows the photocurrent generated by the (12/13)-ds-DNA linked to the CdS–NPs in the presence of the reduced intercalator (15) under conditions where the electrode is biased at −0.4 V (vs. SCE) and the system is exposed to air (oxygen). Several complementary control experiments reveal the important features of the resulting photocurrent: (i) The photocurrent is generated only in the presence of oxygen, and it is totally blocked under inert argon environment. (ii) In contrast to the anodic photocurrent observed in the previous system, a cathodic photocurrent is observed under O_2. (iii) The photocurrent in the system is fully blocked when the potential applied on the electrode is switched to 0 V, a value that retains the intercalator units in their oxidized state (14). These results were rationalized in terms of an electron transfer from the electrode through the reduced intercalator units to the valence-band holes generated upon the photoexcitation of the semiconductor. At the bias potential of −0.4 V (vs. SCE), the intercalator units exist in their reduced leuco form (15) that exhibit electron donating properties, Scheme 5(B). Photoexcitation of the CdS–NPs yields the electron-hole pairs in the conduction-band and valence-band, respectively. The transport of the conduction-band electrons to oxygen with the concomitant transport of electrons from the reduced intercalator units to the valence-band holes completes the cycle for the generation of the photocurrent. The fact that the electrode potential retains the intercalator units in their reduced state and the infinite availability of the electron acceptor (O_2) yields the steady-state anodic photocurrent in the system. Thus, the introduction of TEOA and oxygen to the electrode modified with (14/15)-DNA duplex and associated CdS–NPs would allow the control of the photocurrent direction by switching the bias potential applied on the electrode. Fig. 8 depicts the potential-induced switching of the photocurrent direction upon switching the electrode potential between −0.4 (cathodic photocurrents) and 0 V (anodic photocurrents), respectively. The photocurrents in the intercalator-functionalized DNA-duplex/CdS–NPs assembly originate from a template effect of the DNA matrix that interlocks the intercalator charge-transporting units in the biopolymer. Such photocurrent-generating systems may find interesting and important future applications. The intercalation of molecular units into DNA was found to be perturbed by single-base mismatches [36]. Thus, the present systems and the resulting photocurrents may be employed as a sensing method of base mismatching in DNA. Furthermore, recent research activities have suggested DNA matrices as active interfaces for the development of logic gates [37,38]. The present systems mimic functions of a logic AND gate. The two input stimuli, light and the applied potential, are needed to yield the photocurrent output. It seems that other logic gates may be formulated on the grounds of this biomolecular–NP configuration.

4. Conclusions

The present article introduced new possibilities to use biomolecule–nanoparticle hybrid systems. The coupling of metal nanoparticles to redox enzymes enabled the accomplishment of the electrical communication between redox proteins and electrodes, and the activation of the biocatalytic functions of the respective enzymes. Such electrically contacted enzyme electrodes may have important applications as biosensors and as active elements in biofuel cells. Furthermore, recent activities in nanobiotechnology attempt to use enzyme–nanoparticle hybrids as functional components to tailor nanoscale enzyme-based field-effect transistors [39]. The methods presented here to structurally align enzymes on the nano-elements, and to electrically communicate the enzymes with the nanoparticles may be the clue to the future engineering of these nanoscale devices. Although, semiconductor quantum dots coupled to proteins/DNA found extensive use in the optical/photonic biosensing systems, the use of semiconductor quantum dots for bioelectronics is at its infancy. One may expect that the modification of quantum dots by biomolecules may alter the interfacial electrical properties of the systems, thus allowing the application of such quantum dots as gate elements in future nanoscale transistors. The coupling of light and electrical energy to these biomolecule–semiconductor quantum dots is

anticipated to establish new bioelectrochemical perspectives in nanobiotechnology.

Acknowledgement

This research is supported by the German–Israeli Program (DIP).

References

[1] E. Katz, I. Willner, Integrated nanoparticle–biomolecule hybrid systems: synthesis, properties and applications, Angew. Chem., Int. Ed. 43 (2004) 6042–6108.
[2] C.M. Niemeyer, Nanoparticles, proteins, and nucleic acids: biotechnology meets materials science, Angew. Chem., Int. Ed. 40 (2001) 4128–4158.
[3] I. Willner, E. Katz, Integration of layered redox-proteins and conductive supports for bioelectronic applications, Angew. Chem., Int. Ed. 39 (2000) 1180–1218.
[4] P.N. Bartlett, P. Tebbutt, R.G. Whitaker, Prog. React. Kinet. 16 (1991) 55–155.
[5] Y. Degani, A. Heller, Direct electrical communication between chemically modified enzymes and metal electrodes. I. Electron transfer from glucose oxidase to metal electrodes via electron relays, bound covalently to the enzyme, J. Phys. Chem. 91 (1987) 1285–1289.
[6] W. Schuhmann, T.J. Ohara, H.-L. Schmidt, A. Heller, Electron transfer between glucose oxidase and electrodes via redox mediators bound with flexible chains to the enzyme surface, J. Am. Chem. Soc. 113 (1991) 1394–1397.
[7] I. Willner, A. Riklin, B. Shoham, D. Rivenzon, E. Katz, Development of novel biosensor enzyme-electrodes: glucose oxidase multilayer arrays immobilized onto self-assembled monolayers on electrodes, Adv. Mater. 5 (1993) 912–915.
[8] A. Heller, Electrical connection of enzyme redox centers to electrodes, J. Phys. Chem. 96 (1992) 3579–3587.
[9] H. Bu, S.R. Mikkelsen, A.M. English, Characterization of a ferrocene-containing polyacrylamide-based redox gel for biosensor use, Anal. Chem. 67 (1995) 4071–4076.
[10] I. Willner, E. Katz, N. Lapidot, P. Baüerle, Bioelectrocatalysed reduction of nitrate utilizing polythiophene bipyridinium enzyme electrodes, Bioelectrochem. Bioenerg. 29 (1992) 29–45.
[11] I. Willner, V. Heleg-Shabtai, R. Blonder, E. Katz, G. Tao, A.F. Bückmann, A. Heller, Electrical wiring of glucose oxidase by reconstitution of FAD-modified monolayers assembled onto Au-electrodes, J. Am. Chem. Soc. 118 (1996) 10321–10322.
[12] M. Zayats, E. Katz, I. Willner, Electrical contacting of glucose oxidase by surface reconstitution of the apo-protein on a relay-boronic acid-FAD cofactor monolayer, J. Am. Chem. Soc. 124 (2002) 2120–2121.
[13] O.A. Raitman, E. Katz, A.F. Bückmann, I. Willner, Integration of polyaniline/polyacrylic acid films and redox-enzymes on electrode supports: an in situ electrochemical/surface plasmon resonance study of the bioelectrocatalyzed oxidation of glucose or lactate in the integrated bioelectrocatalytic systems, J. Am. Chem. Soc. 124 (2002) 6487–6496.
[14] O.A. Raitman, F. Patolsky, E. Katz, I. Willner, Electrical contacting of glucose dehydrogenase by the reconstitution of a pyrroloquinoline quinone-functionalized polyaniline film associated with an Au-electrode: An in situ SPR-electrochemical study, Chem. Commun. (2002) 1936–1937.
[15] Y. Xiao, F. Patolsky, E. Katz, J.F. Hainfeld, I. Willner, 'Plugging into enzymes': nanowiring of redox-enzymes by a gold nanoparticle, Science 299 (2003) 1877–1881.
[16] C. Bourdillon, C. Demaille, J. Gueris, J. Moiroux, J.M. Savéant, A fully active monolayer enzyme electrode derivatized by antigen–antibody attachment, J. Am. Chem. Soc. 115 (1993) 12264–12269.
[17] M. Zayats, E. Katz, R. Baron, I. Willner, Reconstitution of apo-glucose dehydrogenase on pyrroloquinoline quinone-functionalized Au nanoparticles yields an electrically contacted biocatalyst, J. Am. Chem. Soc. 127 (2005) 12400–12406.
[18] F. Patolsky, Y. Weizmann, I. Willner, Long-range electrical contacting of redox enzymes by SWCNT connectors, Angew. Chem., Int. Ed. 43 (2004) 2113–2117.
[19] E Granot, E. Katz, B. Basner, I. Willner, Enhanced bioelectrocatalysis using Au-nanoparticle/ polyaniline hybrid systems in thin films and microstructured rods assembled on electrodes, Chem. Mater. 17 (2005) 4600–4609.
[20] R.R. Breaker, DNA enzymes, Nat. Biotechnol. 15 (1997) 427–431.
[21] R.R. Breaker, Catalytic DNA: in training and seeking employment, Nat. Biotechnol. 17 (1999) 422–423.
[22] G.M. Emilsson, R.R. Breaker, Deoxyribozymes: new activities and new applications, Cell Mol. Life Sci. 59 (2002) 596–607.
[23] P. Travascio, Y. Li, D. Sen, DNA-enhanced peroxidase activity of a DNA aptamer–hemin complex, Chem. Biol. 6 (1998) 505–517.
[24] P. Travascio, P.K. Witting, A.G. Mauk, D. Sen, The peroxidase activity of a hemin–DNA oligonucleotide complex: free radical damage to specific guanine bases of the DNA, J. Am. Chem. Soc. 123 (2001) 1337–1348.
[25] Y. Xiao, V. Pavlov, T. Niazov, A. Dishon, M. Kotler, I. Willner, Catalytic beacons for the detection of DNA and telomerase activity, J. Am. Chem. Soc. 126 (2004) 7430–7431.
[26] Y. Xiao, V. Pavlov, R. Gill, T. Bourenko, I. Willner, Lighting up biochemiluminescence by the surface self-assembly of DNA–hemin complexes, ChemBioChem 5 (2004) 374–379.
[27] T. Niazov, V. Pavlov, Y. Xiao, R. Gill, I. Willner, DNAzyme-functionalized Au nanoparticles for the amplified detection of DNA or telomerase activity, Nano Lett. 4 (2004) 1683–1687.
[28] M. Bruchez Jr., M. Moronne, P. Gin, S. Weiss, A.P. Alivisatos, Semiconductor nanocrystals as fluorescent biological labels, Science 281 (1998) 2013–2016.
[29] D. Gerion, W.J. Parak, S.C. Williams, D. Zanchet, C.M. Micheel, A.P. Alivisatos, Sorting fluorescent nanocrystals with DNA, J. Am. Chem. Soc. 124 (2002) 7070–7074.
[30] W.C.W. Chan, S. Nie, Quantum dot bioconjugates for ultrasensitive nonisotopic detection, Science 281 (1998) 2016–2018.
[31] F. Patolsky, R. Gill, Y. Weizmann, T. Mokari, U. Banin, I. Willner, Lighting-up the dynamics of telomerization and DNA replication by CdSe–ZnS quantum dots, J. Am. Chem. Soc. 125 (2003) 13918–13919.
[32] V. Pardo-Yissar, E. Katz, J. Wasserman, I. Willner, Acetylcholine esterase-labeled CdS nanoparticles on electrodes: photoelectrochemical sensing of the enzyme inhibitors, J. Am. Chem. Soc. 125 (2003) 622–623.
[33] T.E. Barman, Enzyme Handbook, vol. 2, Springer-Verlag, New York, 1969, pp. 508–509.
[34] R. Gill, F. Patolsky, E. Katz, I. Willner, Electrochemical control of the photocurrent direction in intercalated DNA/CdS nanoparticle systems,, Angew. Chem. Int. Ed. 44 (2005) 4554–4557.
[35] D. Porath, G. Cuniberti, R. Di Felice, Charge transport in DNA-based devices, Top. Curr. Chem. 237 (2004) 183–227.
[36] S.O. Kelley, E.M. Boon, J.K. Barton, N.M. Jackson, M.G. Hill, Single-base mismatch detection based on charge transduction through DNA, Nucleic Acids Res. 27 (1999) 4830–4837.
[37] Y. Weizmann, R. Elnathan, O. Lioubashevski, I. Willner, Endonuclease-based logic gates and sensors using magnetic force-amplified readout of DNA scission on cantilevers, J. Am. Chem. Soc. 127 (2005) 12666–12672.
[38] A. Okamoto, K. Tanaka, I. Saito, DNA logic gates, J. Am. Chem. Soc. 126 (2004) 9458–9463.
[39] J.J. Xu, W. Zhao, X.L. Luo, H.Y. Chen, A sensitive biosensor for lactate based on layer-by-layer assembling MnO_2 nanoparticles and lactate oxidase on ion-sensitive field-effect transistors, Chem. Commun. (2005) 792–794.